D3Targets-2019-nCoV: A web server to identify potential targets for antivirals against 2019-nCoV

Yulong Shi[1,2,#], Xinben Zhang[1,#], Kaijie Mu[1,3,#], Cheng Peng[1,2,#], Zhengdan Zhu[1,2], Xiaoyu Wang[1], Yanqing Yang[1,2], Zhijian Xu[1,2,*], Weiliang Zhu[1,2,*]

[1]CAS Key Laboratory of Receptor Research; Drug Discovery and Design Center, Shanghai Institute of Materia Medica, Chinese Academy of Sciences, Shanghai, 201203, China

[2]School of Pharmacy, University of Chinese Academy of Sciences, No.19A Yuquan Road, Beijing, 100049, PR China

[3]Nano Science and Technology Institute, University of Science and Technology of China, Suzhou, Jiangsu, 215123, China.

[#]These authors contributed equally to this work.

[*]To whom correspondence should be addressed.

Phone: +86-21-50806600-1201 (Z.X.), +86-21-50805020 (W.Z.),

E-mail: zjxu@simm.ac.cn (Z.X.), wlzhu@simm.ac.cn (W.Z.).

ORCID:

Zhijian Xu: 0000-0002-3063-8473

Weiliang Zhu: 0000-0001-6699-5299

Abstract

2019-nCoV has caused more than 560 deaths as of 6 February 2020 worldwide, mostly in China. Although there are no effective drugs approved, many clinical trials are incoming or ongoing in China which utilize traditional chinese medicine or modern medicine. Moreover, many groups are working on the cytopathic effect assay to fight against 2019-nCoV, which will result in compounds with good activity yet unknown targets. Identifying potential drug targets will be of great importance to understand the underlying mechanism of how the drug works. Here, we compiled the 3D structures of 17 2019-nCoV proteins and 3 related human proteins, which resulted in 208 binding pockets. Each submitted compound will be docked to these binding pockets by the docking software smina and the docking results will be presented in ascending order of compound-target interaction energy (kcal/mol). We hope the computational tool will shed some light on the potential drug target for the identified antivirals. D3Targets-2019-nCoV is available free of charge at https://www.d3pharma.com/D3Targets-2019-nCoV/D3Docking/index.php.

1. Introduction

2019-nCoV[1-3] has caused more than 360 deaths as of 3 February 2020 worldwide, mostly in China. However, no drug has been approved to be effective, although there are some promising results. For example, intravenous treatment of remdesivir is very helpful to improve the clinical condition for the first confirmed patient of 2019-nCoV infection in the United States, although the safety and efficacy are still need to be tested in randomized controlled trials.[4] In addition, there are many incoming or ongoing clinical studies in China (Table 1), probably from the experience to combat severe acute respiratory syndrome-related coronavirus (SARS-CoV). However, most of the targets are unknown. Moreover, many groups are working on the cytopathic effect assay to fight against 2019-nCoV, which will result in compounds with good activity yet unknown targets. Identifying potential drug targets will be of great importance to understand the underlying mechanism of how the drug works. Here, we constructed a docking web server, namely D3Targets-2019-nCoV, including the 3D structures of the 2019-nCoV proteins and the related human proteins from homology modelling or crystal experiments. Each submitted active compound will be docked to all the models and we hope that the docking results will shed some light on the potential target identification.

Table 1. The coming or ongoing clinical studies against 2019-nCoV from Chinese Clinical Trial Registry. [a]

Registration number	Date of Registration	Intervention
ChiCTR2000029518	2020-02-03	TCM clinical prescription combined with the western medicine treatment
ChiCTR2000029496	2020-02-03	Recombinant cytokine gene-derived protein injection
ChiCTR2000029493	2020-02-02	Traditional Chinese Medicine + basic western medical therapies
ChiCTR2000029487	2020-02-02	Oral Gubiao Jiedu Ling Chinese medicine (Traditional Chinese Medicine)
ChiCTR2000029468	2020-02-02	Lopinavir/litonavir (LPV/r) + emtritabine (FTC)/ Tenofovir alafenamide Fumarate tablets (TAF) in combination
ChiCTR2000029461	2020-02-02	TCM decoctions+basic conventional therapy

ChiCTR2000029439	2020-02-01	TCM standard decoctions+basic western medical therapies
ChiCTR2000029438	2020-02-01	Conventional medicine + TCM
ChiCTR2000029436	2020-02-01	TCM syndrome differentiation treatment + Western medicine treatment
ChiCTR2000029435	2020-02-01	Traditional Chinese medicine
ChiCTR2000029434	2020-02-01	Lian-Hua Qing-Wen Capsule/Granule (TCM)+Routine treatment
ChiCTR2000029432	2020-02-01	Tanreqing Injection (TCM)
ChiCTR2000029431	2020-02-01	Critical Treatment in Critical Period + Ankylosaurus+M1 (type I macrophage) suppression therapy
ChiCTR2000029418	2020-01-30	Combined Treatment of Chinese medicine and western medicine
ChiCTR2000029400	2020-01-29	Traditional Chinese medicine treatment
ChiCTR2000029387	2020-01-28	Ribavirin + Interferon alpha-1b; lopinavir / ritonavir + interferon alpha-1b; Ribavirin + LPV/r+Interferon alpha-1b
ChiCTR2000029386	2020-01-28	Adjunctive Corticosteroid Therapy
ChiCTR2000029381	2020-01-27	Xuebijing Injiection (TCM)
ChiCTR2000029308	2020-01-23	Lopinavir-ritonavir tablets + interferon-α2b

[a] Access to http://www.chictr.org.cn/enIndex.aspx on 2020-02-03.

2. Materials and methods

2.1 Homology modelling. 21 severe acute respiratory syndrome-related coronavirus (SARS-CoV) 3D structures were downloaded from protein data bank[5] (PDB IDs: 5Y3E, 2XYR, 2H85, 5NFY, 6JYT, 6NUR, 1UW7, 1QZ8, 2AHM, 1YSY, 1Z1I, 2Z9J, 3E9S, 2HSX, 5X5B, 5X58, 5X29, 2MM4, 1YO4, 2OFZ, 2JIB) and served as templates to build the corresponding 2019-nCoV models in SWISS-MODEL server by "user template" mode.[6]

Magnesium ions (Mg^{2+}) are essential for the RNA-dependent RNA polymerase (RdRp). Therefore, for 2019-nCoV RdRp, we modelled two Mg^{2+} from the superimposition of the HCV RdRp (PDB ID: 1NB6[7]) palm domain to 2019-nCoV RdRp palm domain.

Transmembrane protease serine 2 is a potential target against 2019-nCoV, with its inhibitor camostat mesylate blocking entry of 2019-nCoV into human cells.[8] We model the protein by robetta.[9]

2.2 Experimental structures. Human ACE2 already has electron microscopy structure. Therefore, it is downloaded from PDB (PDB ID: 6ACG) and used for molecular docking.

2.3 Detection of potential binding pockets. Since most of the drug binding pockets of 2019-nCoV proteins are unknown and very difficult to be obtained from experiments in a short time, we applied the D3Pockets web server[10] (https://www.d3pharma.com/D3Pocket/index.php) to systematically analyze the potential binding pockets of each protein. Due to the irregular shape of the predicted binding pockets, we used cuboid pseudo-pocket volume (PPV) to characterize the size of protein pockets by Eq. 1. Once submitting hydrogenated homology-modeled proteins on the D3pockets web server, the PPV and coordinates of predicted binding pockets in proteins could be calculated, among which pockets with the PPV greater than 200 Å^3 are selected for molecular docking.

$$PPV = (X_{max} - X_{min}) * (Y_{max} - Y_{min}) * (Z_{max} - Z_{min}) \quad (1)$$

where X_{max}, X_{min} are the maximum and minimum values of the X coordinate in the pocket file, which was downloaded from the D3pockets web server; Y_{max}, Y_{min} are the maximum and minimum values of the Y coordinate in the pocket file; Z_{max}, $Z_{min}$are the maximum and minimum values of the Z coordinate in the pocket file.

It is critical to choose appropriate docking box parameters for accurate prediction in molecular docking. Based on the coordinate file of predicted binding pockets by D3pockets, the center of the docking box is obtained by Eq. 2, and the size of the docking box is obtained by Eq. 3.

$$(x, y, z) = \left(\frac{X_{max}+X_{min}}{2}, \frac{Y_{max}+Y_{min}}{2}, \frac{Z_{max}+Z_{min}}{2}\right) \quad (2)$$

$$(a, b, c) = (X_{max} - X_{min} + 10, Y_{max} - Y_{min} + 10, Z_{max} - Z_{min} + 10) \quad (3)$$

where x, y, z are the three-dimensional coordinate center of the docking box. a, b, c are the width of the docking box.

2.4 Molecular dynamics of 2019-nCoV M^{pro}. The details of velocity-scaling optimized replica exchange molecular dynamics (vsREMD) method have been

described in our previous study.[11] Briefly, in the vsREMD, a set of replicas are simulated in explicit solvent environment at different temperatures, but exchange between neighboring replicas solely utilizes the sum of intra-protein interaction (P_{pp}) and protein-solvent interaction (P_{pw}) as the criterion by the following equation:

$$\omega(1 \leftrightarrow 2) = min\left(1, exp\left(\Delta\beta\Delta(P_{pp} + P_{pw})\right)\right) \quad (4)$$

where β is the inverse of temperature $1/k_B$T. To obtain the correct ensemble after exchange moves between replica 1 and replica 2, the vsREMD uses Eq.5 & 6 below to rescale uniformly the velocities of all particles,

$$\hat{v}^{(1\to2)} = v^{(2)}\sqrt{\frac{E_{kin}^{(1)} - \Delta P_{ww}}{E_{kin}^{(2)}}} \quad (5)$$

$$\hat{v}^{(2\to1)} = v^{(1)}\sqrt{\frac{E_{kin}^{(2)} + \Delta P_{ww}}{E_{kin}^{(1)}}} \quad (6)$$

where $v^{(1)}$ and $E_{kin}^{(1)}$ are the velocities and kinetic energies of replica 1 before exchange, respectively; $\hat{v}^{(1\to2)}$ is the velocities replica 1 after exchange. The same meaning for replica 2.

The initial structure of the 2019-nCoV M^{pro} was obtained from homology modelling with 1Z1I as template. AMBER99SB*-ILDNP[12] force field was used to model the protein. The simulation system was solvated in a cubic box of TIP3P water molecules with a 10.0 Å buffer along each dimension. To remove bad contacts formed during the system preparation, the simulation system was minimized using steepest descent algorithm. Then the system was heated to 300 K from 0 K in 2 ns with a harmonic restraint (10 kcal·mol^{-1}·Å^{-2}) for the solute. The bonds connecting hydrogen atoms was constrained by the LINCS algorithm[13] and the time step was set to 2.0 fs. The long-range electrostatic interactions were treated by Particle mesh Ewald (PME)[14] with the non-bonded cutoff of 12 Å. The vsREMD was run at 24 different temperatures from 300 to 450 K (300.0, 305.3, 310.8, 316.3, 321.9, 327.6, 333.5, 339.4, 345.4, 351.6, 357.8, 364.2, 370.7, 377.3, 384.0, 390.8, 397.8, 404.8, 412.0, 419.4, 426.8, 434.4, 442.1, 450.0). Exchanges were attempted every 1000 steps. For each replica, the overall simulation time lasted for 50 ns.

2.5 Molecular docking. Hydrogens were added to the homology models by pdb2pqr (--ff=amber --ffout=amber --chain --with-ph=7).[15] The homology models are converted to pdbqt format by prepare_receptor4.py script in MGLToos version 1.5.6.[16] The pockets generated from D3Pockets are used to define the grid. For each small molecule submitted for identifying potential targets, prepare_ligand4.py script in MGLToos version 1.5.6 is used to convert its sdf or mol2 files to pdbqt format.[16] All the docking simulations will be performed by smina,[17] which is a fork of AutoDock Vina[18] with improving scoring and minimization. The random seed was explicitly set to 1 (seed). The exhaustiveness of the global search was set to 8 (exhaustiveness) and at most 1 binding mode was generated for each small molecule against one homolog model (num_modes).

For the docking against RdRp, the interaction between Mg^{2+} and oxygen could not be handled by the default scoring function. Hence, a custom scoring function (-0.3 atom_type_gaussian(t1=Magnesium, t2=OxygenXSAcceptor, o=0, _w=3, _c=8)) is applied.

3. Results and discussion

3.1 Overview of the D3Targets-2019-nCoV database. The 2019-nCoV structure-related proteins and other important proteins on the D3Targets-2019-nCoV database are summarized in Table 2, involving the protein name, number of pockets, pocket code with ligand, etc. The database contains a total of 20 proteins, including proteins in different oligomer states and open / close states.

Table 2. Info on the D3Targets-2019-nCoV database.

Protein Number	Protein Name	Protein ID	Number of Pockets [a]	Pocket Code with Ligand [b]	PDB ID [c]	Organism
1	Host translation inhibitor nsp1	QHD43415.1	3	/ [d]	2HSX	2019-nCoV
2	Papain-like proteinase--Monomer	QHD43415.1	6	1	3E9S	2019-nCoV

2	Papain-like proteinase--Dimer	QHD43415.1	9	1	5Y3E	2019-nCoV
3	3C-like proteinase--Monomer	QHD43415.1	4	2	1Z1I	2019-nCoV
3	3C-like proteinase--Dimer	QHD43415.1	6	3, 4	2Z9J	2019-nCoV
4	Non-structural protein 7	QHD43415.1	1	/	1YSY	2019-nCoV
5	Non-structural protein 8	QHD43415.1	1	/	2AHM	2019-nCoV
6	Non-structural protein 9--Monomer	QHD43415.1	3	/	1UW7	2019-nCoV
6	Non-structural protein 9--Dimer	QHD43415.1	7	/	1QZ8	2019-nCoV
7	Non-structural protein 10	QHD43415.1	3	/	5NFY	2019-nCoV
8	RdRp	QHD43415.1	10	/	6NUR	2019-nCoV
9	Helicase	QHD43415.1	11	/	6JYT	2019-nCoV
10	Helicase—Dimer	QHD43415.1	25	/	6JYT	2019-nCoV
11	Guanine-N7 methyltransferase	QHD43415.1	13	1	5NFY	2019-nCoV
12	Uridylate-specific endoribonuclease	QHD43415.1	7	/	2H85	2019-nCoV
13	2'-O-methyltransferase	QHD43415.1	5	1	2XYR	2019-nCoV
14	ORF7a protein	QHD43421.1	1	/	1YO4	2019-nCoV
15	Spike protein--Close	QHD43416.1	25	/	5X58	2019-nCoV
15	Spike protein--Open	QHD43416.1	28	/	5X5B	2019-nCoV
16	Envelope protein--Monomer	QHD43418.1	1	/	2MM4	2019-nCoV
16	Envelope protein--Pentamer	QHD43418.1	2	/	5X29	2019-nCoV
17	Nucleocapsid phosphoprotein--C terminal	QHD43423.2	1	/	2JIB	2019-nCoV
17	Nucleocapsid phosphoprotein--N terminal	QHD43423.2	4	/	2OFZ	2019-nCoV
18	Angiotensin converting enzyme 2	AAT45083.1	11	1	6ACG	human
19	Cathepsin L	AAN87068.1	11	/	1CS8	human
20	Transmembrane	AAD37117.1	10	/	/	human

protease serine 2

[a] Number of Pockets: the number of potential binding pockets on the protein with the PPV greater than 200 $Å^3$.

[b] Pocket code with ligand: For each protein, all ligand binding sites of homologous proteins with sequence similarities greater than 80% are mapped to the pocket codes generated by the D3Pockets.

[c] PDB ID: For 2019-nCoV proteins and Cathepsin L, the PDB ID refers to the template used for homology modeling. For angiotensin converting enzyme 2, the PDB ID refers to the crystal structure downloaded from PDB used for molecular docking.

[d] Not available.

3.2 Two potential allosteric binding pocket in 2019-nCoV M^{pro}. 2019-nCoV M^{pro} is a promising target to treat the disease.[19] Based on the vsREMD simulation trajectories at 300 K, we applied D3Pockets to explore the dynamic properties of potential pockets in 2019-nCoV M^{pro}. As shown in Figure 1, there are grid points colored from blue to red that compose a pocket. The more red the grid points are, the more stable the subpocket region composed of the points are found throughout the MD trajectory. Therefore, for 2019-nCoV M^{pro}, four relatively stable pockets are observed (Figure 1). Pocket 1, which the intrinsic ligand binds to, has more stable points than Pockets 2, 3, and 4. Pocket 2, which is far from Pocket 1, has a positive volume correlation (0.60) with Pocket 1 (substrate binding site), showing that when Pocket 1 gets bigger, Pocket 2 gets bigger as well (Figure 2A). Similarly, Pocket 3 also has a positive volume correlation (0.69) with Pocket 1 (Figure 2B). There is no correlation between Pockets 1, and 4. It is well known that a pocket with strong correlation with the substrate binding pocket could be used to discovery and design allosteric compounds. Therefore, one can conclude that Pockets 2 and 3 are two potential allosteric binding pockets, which are included in the D3Targets-2019-nCoV web server.

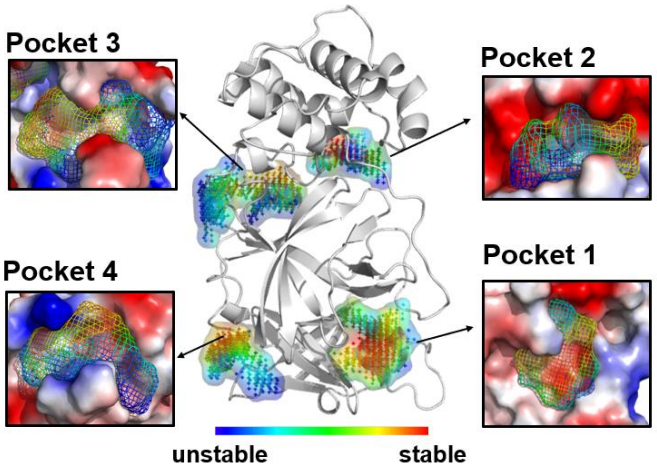

Figure 1. Pocket stability in 2019-nCoV M^{pro}. The protein and the binding pockets are shown in PyMOL.[20]

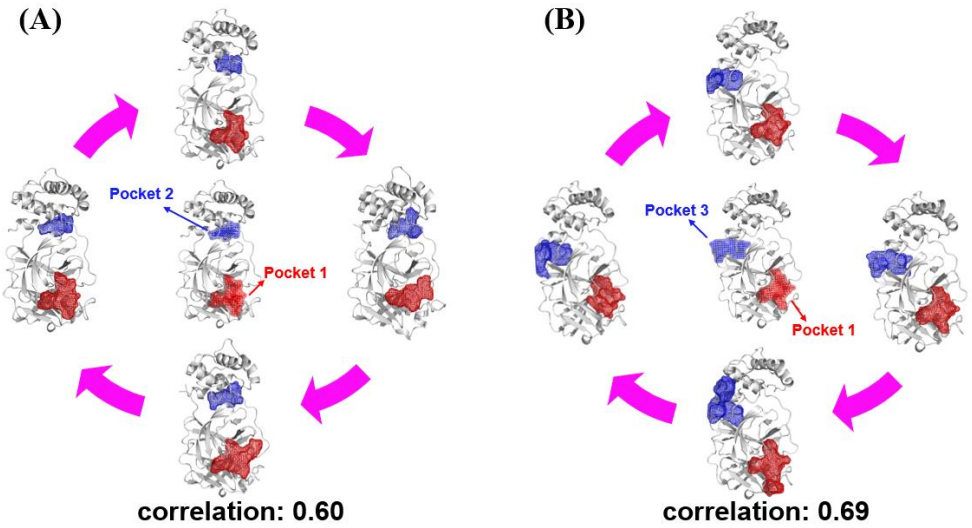

Figure 2. Pocket correlation in 2019-nCoV M^{pro}.

3.3 Input and output.

The input small molecule file should be in sdf or mol2 format. Although we could generate 3D structures from the 2D coordinates by Open Babel[21], the chiral properties might be wrong in the conversion process. Therefore, we strongly recommend the users submitting 3D chemical structure, especially for the compounds with at least one chiral center.

To make the result only visible to a specific user, the user should register, which is free of charge. Otherwise, the docking result will be publicly visible. After registration, the user can login to upload the small molecule. In the case of the users are interested

in some proteins, the target list is customized to be selected manually, while the default is to select all the proteins.

The output is presented in ascending order of compound-target interaction energy (kcal/mol). The docking results could be download from the server as an archive file.

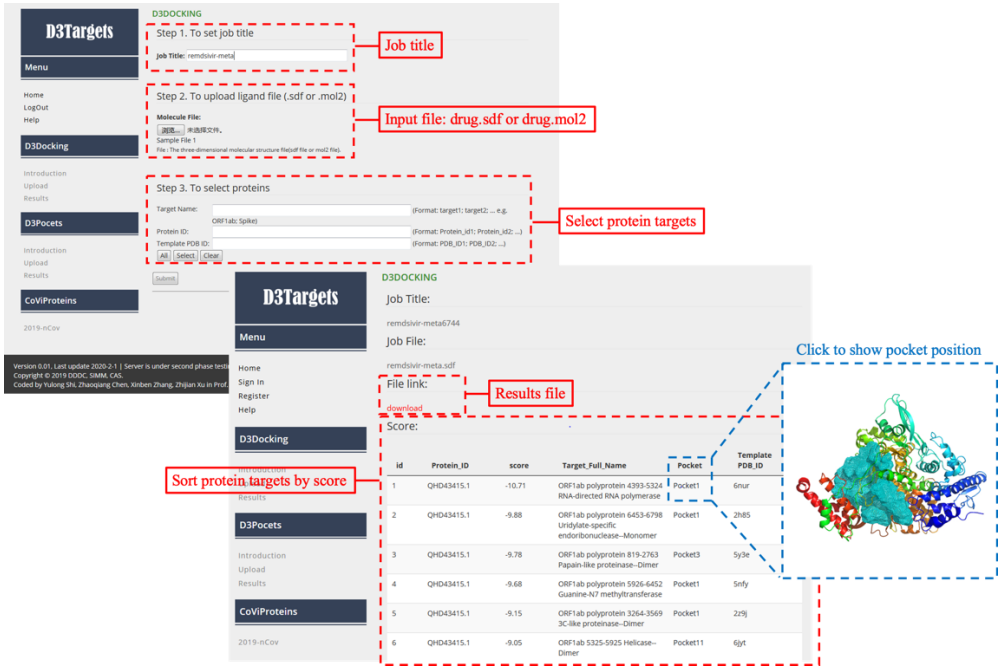

Figure 3. Graphical interface for input and output of D3Targets-2019-nCoV.

3.4 Case study. In order to explore the prediction power of D3Targets-2019-nCoV, remdesivir is used as an example, which is a RdRp inhibitor and is reported to be effective in inhibiting SARS-Cov and 2019-nCoV in vitro[22, 23]. It should be noted that remdesivir is a prodrug, and the active form is the transformed nucleoside triphosphate (NTP, Figure).[24] Therefore, NTP is submitted to D3Targets-2019-nCoV for the target prediction.

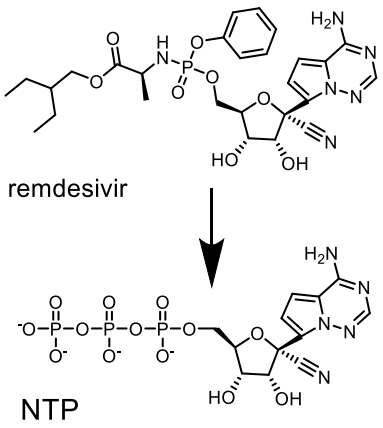

Figure 4. Remdesivir is converted to its pharmacologically active NTP in human cells.

Table 3 shows the top 10 binding pockets and corresponding docking scores for NTP. As the target of remdesivir, RdRp has a score of -10.71 kcal/mol in Pocket 1, which ranks 1st among all protein pockets (20 proteins, 208 pockets), demonstrating the predictive power of D3Targets-2019-nCoV. However, it should be noted that docking score alone does not perform very well in our experience and we recommend the users to check the top 10% docking results carefully to find the real target.

Table 3. Top 10 potential binding pockets and their docking scores for NTP.

Item	Protein	State	Pocket code	Docking score
1	RNA-directed RNA polymerase		1	-10.71
2	Uridylate specific endoribonuclease		1	-9.88
3	Papain-like proteinase	Dimer	3	-9.78
4	Papain like proteinase	Dimer	2	-9.75
5	Guanine-N7 methyltransferase		1	-9.68
6	3C-like proteinase	Dimer	1	-9.15
7	Papain-like proteinase	Dimer	1	-9.08
8	Helicase	Dimer	11	-9.05
9	2'-O-methyltransferase		1	-8.91
10	Transmembrane protease serine 2		2	-8.81

The superiority to use the docking method to predict the target is that docking result shows the binding mode of the compound into the target, which is very useful for the mutagenesis validation. According to the binding mode of NTP to the RdRp (Figure), hydrogen bonds and electrostatic interactions play an important role in the high affinity. In detail, the hydrogen bonds between NTP and some crucial residues in RdRp, such as GLU-811, TRP-800 and SER-814, may determine the ability to suppress 2019-nCoV. Besides, there is a strong electrostatic attraction between the phosphate group of NTP with two Mg^{2+}, which may be helpful to explain the preference of RdRp for nucleotide analogs. The docking result of NTP is in consistent with the experiment, demonstrating the accuracy and robustness of D3Targets-2019-nCoV in exploring drug targets.

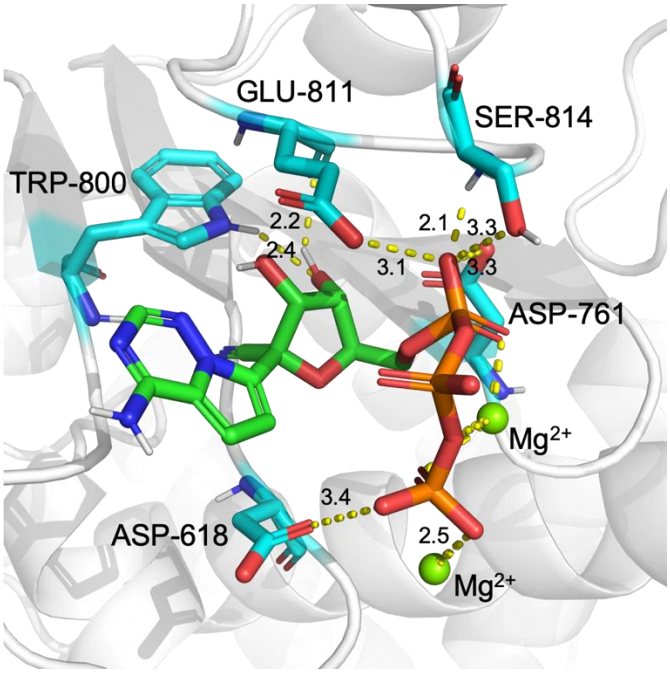

Figure 5. Binding mode of NTP to the RdRp from the docking simulation.

4. Conclusions

2019-nCoV has caused more than 560 deaths as of 6 February 2020 worldwide, mostly in China. Although there are no effective drugs approved, many clinical trials are incoming or ongoing in China which utilize traditional chinese medicine or modern medicine. Moreover, many groups are working on the cytopathic effect assay to fight against 2019-nCoV, which will result in compounds with good activity yet unknown targets. Therefore, identifying potential drug targets will be of great importance to develop effective drugs. Here, we compiled 3D structures of 17 2019-nCoV proteins and 3 related human proteins, which resulted in 208 binding pockets. We run vsREMD simulation on M^{pro}, a promising target against 2019-nCoV, and find two pockets of high druggability. Each submitted compound will be docked to these binding pockets by smina and the docking results will be presented in ascending order of compound-target interaction energy (kcal/mol). When testing an antiviral against 2019-nCoV, i.e., remdesivir, the proposed target RdRp ranks 1st, demonstrating the usefulness of the computational tool. We hope D3Targets-2019-nCoV will shed some light on the potential drug target for the identified antivirals, which is available free of charge at https://www.d3pharma.com/D3Targets-2019-nCoV/D3Docking/index.php.

Acknowledgments

This work was supported by the National Key R&D Program of China (2016YFA0502301 & 2017YFB0202601).

References

1. Zhu, N.; Zhang, D.; Wang, W.; Li, X.; Yang, B.; Song, J.; Zhao, X.; Huang, B.; Shi, W.; Lu, R.; Niu, P.; Zhan, F.; Ma, X.; Wang, D.; Xu, W.; Wu, G.; Gao, G. F.; Tan, W., A Novel Coronavirus from Patients with Pneumonia in China, 2019. *The New England journal of medicine* **2020**.
2. Zhou, P.; Yang, X.-L.; Wang, X.-G.; Hu, B.; Zhang, L.; Zhang, W.; Si, H.-R.; Zhu, Y.; Li, B.; Huang, C.-L.; Chen, H.-D.; Chen, J.; Luo, Y.; Guo, H.; Jiang, R.-D.; Liu, M.-Q.; Chen, Y.; Shen, X.-R.; Wang, X.; Zheng, X.-S.; Zhao, K.; Chen, Q.-J.; Deng, F.; Liu, L.-L.; Yan, B.; Zhan, F.-X.; Wang, Y.-Y.; Xiao, G.-F.; Shi, Z.-L., A pneumonia outbreak associated with a new coronavirus of probable bat origin. *Nature* **2020**.
3. Wu, F.; Zhao, S.; Yu, B.; Chen, Y.-M.; Wang, W.; Song, Z.-G.; Hu, Y.; Tao, Z.-W.; Tian, J.-H.; Pei, Y.-Y.; Yuan, M.-L.; Zhang, Y.-L.; Dai, F.-H.; Liu, Y.; Wang, Q.-M.; Zheng, J.-J.; Xu, L.; Holmes, E. C.; Zhang, Y.-Z., A new coronavirus associated with human respiratory disease in China. *Nature* **2020**.
4. Holshue, M. L.; DeBolt, C.; Lindquist, S.; Lofy, K. H.; Wiesman, J.; Bruce, H.; Spitters, C.; Ericson, K.; Wilkerson, S.; Tural, A.; Diaz, G.; Cohn, A.; Fox, L.; Patel, A.; Gerber, S. I.; Kim, L.; Tong, S.; Lu, X.; Lindstrom, S.; Pallansch, M. A.; Weldon, W. C.; Biggs, H. M.; Uyeki, T. M.; Pillai, S. K.; Washington State -nCo, V. C. I. T., First Case of 2019 Novel Coronavirus in the United States. *N. Engl. J. Med.* **2020**.
5. Burley, S. K.; Berman, H. M.; Bhikadiya, C.; Bi, C.; Chen, L.; Di Costanzo, L.; Christie, C.; Dalenberg, K.; Duarte, J. M.; Dutta, S.; Feng, Z.; Ghosh, S.; Goodsell, D. S.; Green, R. K.; Guranović, V.; Guzenko, D.; Hudson, B. P.; Kalro, T.; Liang, Y.; Lowe, R.; Namkoong, H.; Peisach, E.; Periskova, I.; Prlić, A.; Randle, C.; Rose, A.; Rose, P.; Sala, R.; Sekharan, M.; Shao, C.; Tan, L.; Tao, Y.-P.; Valasatava, Y.; Voigt, M.; Westbrook, J.; Woo, J.; Yang, H.; Young, J.; Zhuravleva, M.; Zardecki, C., RCSB Protein Data Bank: biological macromolecular structures enabling research and education in fundamental biology, biomedicine, biotechnology and energy. *Nucleic Acids Res.* **2018,** *47* (D1), D464-D474.
6. Waterhouse, A.; Bertoni, M.; Bienert, S.; Studer, G.; Tauriello, G.; Gumienny, R.; Heer, F. T.; de Beer, T. A P.; Rempfer, C.; Bordoli, L.; Lepore, R.; Schwede, T., SWISS-MODEL: homology modelling of protein structures and complexes. *Nucleic Acids Res.* **2018,** *46* (W1), W296-W303.

7. O'Farrell, D.; Trowbridge, R.; Rowlands, D.; Jager, J., Substrate complexes of hepatitis C virus RNA polymerase (HC-J4): structural evidence for nucleotide import and de-novo initiation. *J. Mol. Biol.* **2003,** *326* (4), 1025-35.
8. Hoffmann, M.; Kleine-Weber, H.; Krueger, N.; Mueller, M. A.; Drosten, C.; Poehlmann, S., The novel coronavirus 2019 (2019-nCoV) uses the SARS-coronavirus receptor ACE2 and the cellular protease TMPRSS2 for entry into target cells. *bioRxiv* **2020**, 2020.01.31.929042.
9. Kim, D. E.; Chivian, D.; Baker, D., Protein structure prediction and analysis using the Robetta server. *Nucleic Acids Res.* **2004,** *32* (Web Server issue), W526-31.
10. Chen, Z.; Zhang, X.; Peng, C.; Wang, J.; Xu, Z.; Chen, K.; Shi, J.; Zhu, W., D3Pockets: A Method and Web Server for Systematic Analysis of Protein Pocket Dynamics. *J. Chem. Inf. Model.* **2019,** *59* (8), 3353-3358.
11. Wang, J.; Peng, C.; Yu, Y.; Chen, Z.; Xu, Z.; Cai, T.; Shao, Q.; Shi, J.; Zhu, W., Exploring Conformational Change of Adenylate Kinase by Replica Exchange Molecular Dynamic Simulation. *Biophys. J.* **2020**.
12. Aliev, A. E.; Kulke, M.; Khaneja, H. S.; Chudasama, V.; Sheppard, T. D.; Lanigan, R. M., Motional timescale predictions by molecular dynamics simulations: case study using proline and hydroxyproline sidechain dynamics. *Proteins* **2014,** *82* (2), 195-215.
13. Hess, B.; Bekker, H.; Berendsen, H. J. C.; Fraaije, J. G. E. M., LINCS: A linear constraint solver for molecular simulations. *J. Comput. Chem.* **1997,** *18* (12), 1463-1472.
14. Darden, T.; York, D.; Pedersen, L., Particle mesh Ewald: An N· log (N) method for Ewald sums in large systems. *J. Chem. Phys.* **1993,** *98*, 10089.
15. Dolinsky, T. J.; Nielsen, J. E.; McCammon, J. A.; Baker, N. A., PDB2PQR: an automated pipeline for the setup of Poisson–Boltzmann electrostatics calculations. *Nucleic Acids Res.* **2004,** *32* (suppl_2), W665-W667.
16. Morris, G. M.; Huey, R.; Lindstrom, W.; Sanner, M. F.; Belew, R. K.; Goodsell, D. S.; Olson, A. J., AutoDock4 and AutoDockTools4: Automated docking with selective receptor flexibility. *J. Comput. Chem.* **2009,** *30* (16), 2785-2791.
17. Koes, D. R.; Baumgartner, M. P.; Camacho, C. J., Lessons Learned in Empirical Scoring with smina from the CSAR 2011 Benchmarking Exercise. *J. Chem. Inf. Model.* **2013,** *53* (8), 1893-1904.
18. Trott, O.; Olson, A. J., AutoDock Vina: Improving the speed and accuracy of docking with a new scoring function, efficient optimization, and multithreading. *J. Comput. Chem.* **2010,** *31* (2), 455-461.
19. Xu, Z.; Peng, C.; Shi, Y.; Zhu, Z.; Mu, K.; Wang, X.; Zhu, W., Nelfinavir was predicted to be a potential inhibitor of 2019-nCoV main protease by an integrative approach combining homology modelling, molecular docking and binding free energy calculation. *bioRxiv* **2020**, 2020.01.27.921627.
20. Schrodinger, LLC, The PyMOL Molecular Graphics System, Version 2.4. 2019.
21. O'Boyle, N. M.; Banck, M.; James, C. A.; Morley, C.; Vandermeersch, T.; Hutchison, G. R., Open Babel: An open chemical toolbox. *J. Cheminform.* **2011,** *3* (1), 33.

22. Agostini, M. L.; Andres, E. L.; Sims, A. C.; Graham, R. L.; Sheahan, T. P.; Lu, X.; Smith, E. C.; Case, J. B.; Feng, J. Y.; Jordan, R.; Ray, A. S.; Cihlar, T.; Siegel, D.; Mackman, R. L.; Clarke, M. O.; Baric, R. S.; Denison, M. R., Coronavirus Susceptibility to the Antiviral Remdesivir (GS-5734) Is Mediated by the Viral Polymerase and the Proofreading Exoribonuclease. *mBio* **2018,** *9* (2).
23. Wang, M.; Cao, R.; Zhang, L.; Yang, X.; Liu, J.; Xu, M.; Shi, Z.; Hu, Z.; Zhong, W.; Xiao, G., Remdesivir and chloroquine effectively inhibit the recently emerged novel coronavirus (2019-nCoV) in vitro. *Cell Res.* **2020**.
24. Warren, T. K.; Jordan, R.; Lo, M. K.; Ray, A. S.; Mackman, R. L.; Soloveva, V.; Siegel, D.; Perron, M.; Bannister, R.; Hui, H. C.; Larson, N.; Strickley, R.; Wells, J.; Stuthman, K. S.; Van Tongeren, S. A.; Garza, N. L.; Donnelly, G.; Shurtleff, A. C.; Retterer, C. J.; Gharaibeh, D.; Zamani, R.; Kenny, T.; Eaton, B. P.; Grimes, E.; Welch, L. S.; Gomba, L.; Wilhelmsen, C. L.; Nichols, D. K.; Nuss, J. E.; Nagle, E. R.; Kugelman, J. R.; Palacios, G.; Doerffler, E.; Neville, S.; Carra, E.; Clarke, M. O.; Zhang, L.; Lew, W.; Ross, B.; Wang, Q.; Chun, K.; Wolfe, L.; Babusis, D.; Park, Y.; Stray, K. M.; Trancheva, I.; Feng, J. Y.; Barauskas, O.; Xu, Y.; Wong, P.; Braun, M. R.; Flint, M.; McMullan, L. K.; Chen, S.-S.; Fearns, R.; Swaminathan, S.; Mayers, D. L.; Spiropoulou, C. F.; Lee, W. A.; Nichol, S. T.; Cihlar, T.; Bavari, S., Therapeutic efficacy of the small molecule GS-5734 against Ebola virus in rhesus monkeys. *Nature* **2016,** *531* (7594), 381-385.